Uludağ Üniversitesi Tıp Fakültesi Dergisi
Journal of Uludağ University Medical Faculty
51 (2) 223-231, 2025
DOI: https://doi.org/10.32708/uutfd.1691390

ORIGINAL RESEARCH

Anti-Fibrotic and Regenerative Potential of Mesenchymal Stem Cell-Derived Exosomes in Cisplatin-Induced Kidney Injury

Halime TOZAK YILDIZ[1], Kübra Tuğçe KALKAN[1], Numan BAYDİLLİ[2], Zeynep Burçin GÖNEN[3], Özge CENGİZ MAT[4], Eda KÖSEOĞLU[4], Gözde Özge ÖNDER[4], Arzu YAY[4]

[1] Department of Histology and Embryology, Faculty of Medicine, Kırşehir Ahi Evran University, Kirsehir, Türkiye.
[2] Department of Urology, Faculty of Medicine, Erciyes University, Melikgazi, Kayseri, Türkiye.
[3] Betül-Ziya Eren Genome and Stem Cell Center (GENKOK), Erciyes University, Melikgazi, Kayseri, Türkiye.
[4] Department of Histology and Embryology, Faculty of Medicine, Erciyes University, Melikgazi, Kayseri, Türkiye.

ABSTRACT

Cisplatin is a widely used chemotherapeutic agent with potent antitumor activity; however, its nephrotoxicity limits clinical use, affecting 30–40% of treated patients. This study aimed to investigate the effects of mesenchymal stem cell-derived exosomes on cisplatin-induced nephrotoxicity and fibrosis in rat kidney tissue. Rats were divided into Control, Cis, Exo, and Cis+Exo groups. Nephrotoxicity was induced by a single dose Cis. Exosomes were isolated using a commercial kit and characterized by nanoparticle tracking analysis. Histopathological evaluations were performed Hematoxylin&Eosin and Periodic Acid-Schiff. Fibrosis markers were assessed by immunohistochemistry. Statistical analyses were conducted using one-way ANOVA and Kruskal-Wallis tests with Bonferroni and Dunn's post-hoc tests, considering $p<0.05$ as statistically significant. In the Cis group, significant tubular degeneration, necrosis, and fibrosis were observed compared to the Control group. TGF-β1, α-SMA, and TLR-4 expressions were markedly increased in the Cis group ($p<0.001$). Exo treatment significantly reduced the expression levels of these fibrosis markers compared to the Cis group (TGF-β1 and TLR-4, $p<0.001$; α-SMA, $p<0.05$). Histopathological analysis revealed that Exo administration mitigated nephrotoxic damage and supported tissue regeneration, with tissue architecture resembling that of the Control group. This study demonstrates that MSC-derived exosomes alleviate not only acute cisplatin-induced injury but also the associated fibrotic response. A single dose of exosome treatment significantly modulated the fibrotic response and reduced oxidative stress-induced damage. These findings indicate that MSC-derived exosomes, known for their regenerative and tissue-repairing properties, also possess significant potential as antifibrotic therapeutic agents, highlighting the need for further research toward clinical applications.

Keywords: Exosomes. Fibrosis. Mesenchymal stem cell. Nephrotoxicity. Cisplatin.

Sisplatinle İndüklenen Böbrek Hasarında Mezankimal Kök Hücre Kökenli Eksozomların Anti-Fibrotik ve Rejeneratif Potansiyeli

ÖZET

Sisplatin, güçlü antitümöral aktiviteye sahip, yaygın olarak kullanılan bir kemoterapi ajanıdır; ancak nefrotoksisite oluşturması, klinik kullanımını sınırlamakta ve tedavi edilen hastaların %30–40'ında görülmektedir. Bu çalışma, mezankimal kök hücre kaynaklı eksozomların, sisplatin ile indüklenen nefrotoksisite ve fibrozis üzerindeki etkilerini sıçan böbrek dokusunda araştırmayı amaçlamıştır. Sıçanlar kontrol, Cis, Exo ve Cis+Exo olmak üzere dört gruba ayrıldı. Nefrotoksisite, tek doz sisplatin uygulanarak indüklendi. Eksozomlar ticari bir kit kullanılarak izole edildi ve nanoparçacık izleme analizi ile karakterize edildi. Histopatolojik değerlendirmeler Hematoksilen&Eozin, Periyodik Asit-Schiff ile yapıldı. Fibrozis belirteçleri immünohistokimyasal boyama ile değerlendirildi. İstatistiksel analizler, çoklu grup karşılaştırmaları için tek yönlü ANOVA ve Kruskal-Wallis testleri kullanılarak, Bonferroni ve Dunn post-hoc testleri ile gerçekleştirildi. $p<0,05$ değeri istatistiksel olarak anlamlı kabul edildi.Cis grubunda, kontrol grubuna kıyasla anlamlı düzeyde tübüler dejenerasyon, nekroz ve fibrozis gözlendi. Histopatolojik analizler, Exo uygulamasının nefrotoksik hasarı azalttığını ve doku rejenerasyonunu desteklediğini, doku mimarisinin Kontrol grubuna benzer hale geldiğini ortaya koydu. TGF-β1, α-SMA ve TLR-4 ekspresyonları Cis grubunda belirgin şekilde artmıştı ($p<0,001$). Exo tedavisi, bu fibrozis belirteçlerinin ekspresyon seviyelerini Cis grubuna göre anlamlı düzeyde azalttı (TGF-β1 ve TLR-4 için $p<0,001$; α-SMA için $p<0,05$). Bu çalışma, MSC kaynaklı eksozomların yalnızca akut sisplatin hasarını değil, aynı zamanda ilişkili fibrotik süreci de hafiflettiğini göstermektedir. Tek doz Exo tedavisi, fibrotik yanıtı anlamlı şekilde modüle etmiş ve oksidatif stres kaynaklı doku hasarını azaltmıştır. Bu bulgular, rejeneratif ve doku onarıcı etkileri iyi bilinen MSC kaynaklı eksozomların, aynı zamanda belirgin bir antifibrotik bir tedavi ajanı olma potansiyeline de sahip olduğunu göstermekte ve klinik uygulamalara yönelik ileri araştırmaların gerekliliğini ortaya koymaktadır**.**

Anahtar Kelimeler: Eksozom. Fibrozis. Mezenkimal kök hücre. Nefrotosisite. Sisplatin.

Date Received: 4.May.2025
Date Accepted: 2.July.2025

Dr. Halime TOZAK YILDIZ
Department of Histology and Embryology,
Faculty of Medicine, Kirsehir Ahi Evran University,
40100 Kirsehir.
Phone: +90 386 280 39 00, 0505 359 53 94
E-mail: htyildiz@ahievran.edu.tr, hhalimeyildiz@hotmail.com

AUTHORS' ORCID INFORMATION
Halime TOZAK YILDIZ: 0000-0003-4310-6238
Kübra Tuğçe KALKAN: 0000- 0001- 7461- 277X
Numan BAYDİLLİ, 0000-0003-1017-3653.
Zeynep Burçin GÖNENÇ: 0000-0003-2725-9330
Özge CENGİZ MAT: 0000-0003-4638-6116
Eda KÖSEOĞLU: 0000-0003-4638-6116
Gözde Özge ÖNDER: 0000-0002-0515-9286
Arzu YAY 0000-0002-0541-8372

Extracellular vesicles (EVs) are lipid bilayered nanovesicles of varying sizes, contents, and mechanisms, secreted by nearly all cell types. Based on current knowledge regarding their biogenesis, these vesicles are classified into two main categories: exosomes (Exo) and microvesicles[1]. Exo are the smallest extracellular carriers, with diameters ranging between 30 and 120 nm, enclosed by a phospholipid bilayer[2]. Owing to their versatile roles in intercellular communication, Exo are critically involved in numerous biological processes, ranging from physiological regulation and disease progression to modulation of immune responses and pathogenesis[3]. Their high biocompatibility, low toxicity, and ability to traverse biological membranes have positioned Exo as a promising tool, particularly in the field of cancer therapy[4]. The biological functions of Exo are determined by the bioactive molecules they carry, including lipids, metabolites, proteins, and nucleic acids, which exert effects on target cells[5]. In this context, Exo are explored in cancer treatment within two main strategies: as carriers for therapeutic agents and as modulators of the tumor microenvironment to inhibit tumor growth and metastasis[3,5].

The kidney is a crucial excretory organ responsible for maintaining homeostasis and receives approximately 25% of the cardiac output. Consequently, it is one of the primary target organs in drug-induced toxicity[6]. The most significant dose-limiting side effect of cisplatin (Cis) is nephrotoxicity[7]. Cis-induced nephrotoxicity is dose-dependent, which in turn limits the drug's therapeutic efficacy[8]. Since Cis is not absorbed through the gastrointestinal tract, it can only be administered intravenously or intraperitoneally[9]. Approximately 90% of Cis binds to plasma proteins, and platinum residues have been reported in renal tissue even four months after administration[10]. The mechanisms underlying Cis nephrotoxicity include oxidative stress, apoptosis, necrosis, inflammation, fibrogenesis, and mitochondrial damage, all of which are interconnected[11]. Following kidney injury, damaged cells secrete various soluble factors that trigger fibroblast activation and inflammatory responses[12]. Renal fibrosis is characterized by persistent fibroblast activation leading to excessive extracellular matrix (ECM) accumulation, which results in scar formation, structural damage to the renal parenchyma, and ultimately, renal dysfunction[4,13]. In this process, transforming growth factor-beta (TGF-β) plays a pivotal role in driving fibrosis through both Smad-dependent and alternative signaling pathways, promoting the differentiation of fibroblasts into myofibroblasts. As a hallmark of myofibroblast activation, alpha-smooth muscle actin (α-SMA) is widely used as a marker for the assessment of fibrogenic activity in various kidney injury models[14]. Additionally, Toll-like receptor 4 (TLR4) has been shown to mediate inflammation-driven fibrosis by activating innate immune signaling pathways, linking tissue injury to fibrotic remodeling[15]. Therefore, in this study, TGF-β1, α-SMA, and TLR4 were selected as key molecular markers to evaluate the antifibrotic effects of exosomes in a cisplatin-induced nephrotoxicity model.

The therapeutic, immunomodulatory, and regenerative effects of mesenchymal stem cells (MSCs) are believed to be mediated predominantly through paracrine mechanisms involving cytokines, growth factors, hormones, and Exo[16]. These molecules promote angiogenesis, stimulate extracellular matrix production, and regulate immune responses by reducing apoptosis and fibrosis[17]. Exo derived from MSCs contributesto maintaining tissue homeostasis and supporting cellular functions by initiating regenerative processes. Compared to MSC transplantation, exosome-based therapies are considered a superior clinical alternative due to their low immunogenicity, high safety profile, absence of tumorigenic potential, and ethical advantages[5,18,19].

Because of their anti-inflammatory, anti-apoptotic, and anti-fibrotic properties, Exo may contribute to the preservation of renal function and the suppression of fibrotic processes. In this context, the therapeutic potential of Exo in cisplatin-induced kidney injury has attracted increasing attention. This study aims to investigate the reparative effects of mesenchymal stem cell-derived Exo on cisplatin-induced renal fibrosis and to highlight the potential of exosome-based therapeutic strategies as a safe and effective alternative to current treatment modalities.

Material and Method

Experimental Groups and Treatment Protocols

The experiments were conducted in accordance with The ARRIVE guidelines (Animal Research: Reporting of In Vivo Experiments). Ethics Committee Approval:

Erciyes University Animal Experiments Local Ethics Committee (decision no: 24/030, date: 07.02.2024). The study does not require patient consent.

The study was initiated with 32 male Wistar albino rats, aged 8 to 10 weeks. The rats were kept in a 25°C room with a 12-hour light/dark cycle, free access to water, and a standard diet from the Experimental and Clinical Research Center at Erciyes University, Kayseri, Turkiye.

In this study, the rats were randomly divided into four groups (n = 8 per group):

Group 1 (Control, C): No treatment was administered.

Group 2 (Exosome, Exo): The group treated with Exo received a single intravenous injection (i.v.) of exosome ($8x10^7$/100 µl) on the sixth day of the experiment[20].

Group 3 (Cisplatin, Cis): The Cis group was administered a single intraperitoneal (i.p.) injection of Cis (7.5mg/kg) (Kocak Pharma, Istanbul, Türkiye) on the first day of the experiment to induce nephrotoxicity[21].

Group 4 (Cisplatin + Exosome, Cis+Exo): Rats were administered a single i.p. injection of Cis (7.5mg/kg) on the first day to induce nephrotoxicity. On the sixth day, a single i.v. dose of Exo ($8x10^7$/100 µl) was administered to the rats.

All procedures were carried out at the same time of day to ensure consistency in experimental conditions. On the 8th day, tissue samples were collected under general anesthesia (xylazine;10 mg/kg, and ketamine;60 mg/kg, i.p.), and the animals were sacrificed.

Surgical Procedure

On the 8th day of the experiment, all groups were anesthetized intraperitoneally with ketamine hydrochloride (60 mg/kg) and xylazine hydrochloride (10 mg/kg, 2% solution). Under sterile conditions, a midline incision was made to perform a laparotomy. After opening the subcutaneous connective tissue and abdominal muscles, the left kidney was carefully dissected. The kidney was then placed in formaldehyde for subsequent histopathological and immunohistochemical evaluations.

Exosome Isolation

MSCs derived from the bone marrow of Wistar albino rats were obtained from the Genome and Stem Cell Center (GENKÖK) at Erciyes University, Türkiye[22]. Exosomes (Exo) were subsequently isolated from the secretomes of these cells Previously isolated and frozen MSCs were thawed in a 37°C water bath and seeded into 75 cm² cell culture flasks (TP Inc, Rochester, NY, USA). When the MSCs reached over 90% confluency, a serum-free medium (MEM-α, Cat. No: BI01-042-1A; Biological Industries, Beit HaEmek, Israel) was added, and the secretomes were collected after 24 hours.

A commercial kit (ExoQuick-TC Exosome Precipitation Solution Kit, Palo Alto, California, United States) was used to perform standard exosome isolation[23]. For exosome isolation, collected secretomes were centrifuged at 3000 × g for 15 minutes, and the supernatants were transferred into sterile tubes. To each 10 ml of supernatant, 2 ml of ExoQuick-TC solution was added, and the mixture was incubated overnight. Following incubation, the ExoQuick-TC/supernatant mixture was centrifuged at 1500 × g for 30 minutes. The supernatants were removed, and the Exo formed a pellet at the bottom of the tube. For exosomal protein analysis, the resulting pellet was resuspended in 100–500 µl of ExoQuick-TC solution. The quantity of Exo was determined using a microvesicle measurement kit (ExoQuick-TC Exosome Precipitation Solution Kit). The average particle size of the secretomes was measured using the Nanoparticle Tracking Analysis system (NTA, Malvern Instrument Nanosight NS300, Malvern, UK). The live particle imaging settings were adjusted according to the manufacturer's software manual (NanoSight NS300 User Manual, MAN0541-01-TR-00, 2017), and the measurements were completed (n = 3). Exosome quantification was performed using the ExoCet Exosome Quantitation Kit (EXOCET96A-1; System Biosciences, Palo Alto, CA, USA) on a Glomax® Multi Detection System microplate reader (Promega, Madison, WI, USA). This kit is an antibody-free, colorimetric enzymatic assay based on the activity of acetylcholinesterase (AChE), an enzyme highly enriched in the exosomal membrane. The enzymatic reaction produces a colorimetric signal that is measured at 405 nm. All absorbance readings were conducted at this wavelength using the Glomax® system. A standard curve was generated from known exosome standards provided with the kit, and exosome concentrations in the samples were calculated accordingly[24]. Exo diluted to a concentration of $8X10^7$ particles/100 µl were injected into the Exo and Cis + Exo groups in the study.

Histopathological Analysis

In order to histologically evaluate kidney defects in each experimental group, tissue samples collected at the end of the experiment were fixed in 10% formaldehyde solution. After 72 hours of fixation, the tissues were washed under running tap water, dehydrated through a graded series of alcohol, cleared in xylene, and embedded in paraffin. Sections of 5 µm thickness were obtained from the paraffin blocks and placed onto slides (Leica, Autocut, 14051956472, Germany). The prepared slides were deparaffinized

using xylene, rehydrated through a graded series of alcohols (100%, 96%, 80%, 70%, 50%), and washed in water following a standard histological staining protocol. For general histological assessment, the sections were stained with Hematoxylin and Eosin (H&E) (Bio-Optica 05-06004/L Harris' Hematoxylin & Bio-Optica 05-10002/L Eosin Y 1%) and Periodic Acid-Schiff (PAS) (Best Lab, Türkiye). After staining, the sections were dehydrated through ascending alcohol series, cleared with xylene, and mounted with coverslips using Entellan. The sections were then evaluated under a light microscope. Degenerative changes in the tubular and intertubular areas were assessed semi-quantitatively. In each kidney section, 10 different fields were evaluated for each damage parameter, and average percentage values within each group were calculated. Histopathological changes were scored as follows: changes observed in less than 25% of tubular epithelial cells were scored as 1 (mild), 25–50% as 2 (moderate), 50–75% as 3 (severe), and 75–100% as 4 (very severe) (absence=0, mild=1, moderate=2, severe=3, very severe=4)[25].

Immunohistochemical Analysis

The immunohistochemical staining kit (Lab VisionTM UltraVisionTM Large Volume Detection System: anti-polyvalent, HRP, TA-125-HL) was used in conjunction with the streptavidin-biotin-peroxidase method. Using this method, the expression levels of fibrotic markers TGF-β1, α-SMA, and TLR4 in kidney tissues were demonstrated immunohistochemically. For immunohistochemical staining, 5 µm sections were obtained from paraffin-embedded blocks prepared by routine processing following 10% formalin fixation. The sections were incubated overnight at 56°C, then deparaffinized in xylene for 15 minutes, dehydrated through descending alcohol series (%99, %96, and %70), and rehydrated by immersion in distilled water for 10 minutes. For antigen retrieval, the sections were boiled in 5% citrate buffer in a microwave oven at 600W for 5 minutes and subsequently washed with PBS. To block endogenous peroxidase activity, the sections were treated with 3% hydrogen peroxide (H_2O_2) for 20 minutes. After washing with PBS, blocking serum was applied at room temperature for 10 minutes to prevent non-specific binding.

The sections were incubated overnight at 4°C with primary antibodies against TGF-β (Proteintech, Cat No. 21898-1-AP, 1:250), α-SMA (Proteintech, Cat No. 80008-1-RR, 1:2500), and TLR-4 (Proteintech, Cat No. 19811-1-AP, 1:400). Following washing, the sections were incubated with a biotinylated secondary antibody for 20 minutes, washed again, and then treated with streptavidin-peroxidase (Thermo Scientific, SHRP248-B) for 20 minutes before a final wash. Diaminobenzidine (DAB) solution was applied, and the tissues were monitored under a light microscope until a visible signal developed, after which all groups were washed simultaneously with tap water.

The sections were counterstained with Mayer's hematoxylin, rinsed with distilled water, passed through ascending alcohol series (5 minutes in each concentration), cleared in xylene for 15 minutes, and finally mounted with Entellan without air bubbles. The immunohistochemically stained sections were examined under a light microscope, and microscopic images were captured from 20 different fields. Immunoreactivity intensities of the targeted markers in the captured images were quantified using the ImageJ software program (NIH, Washington, USA), and the results were evaluated[26].

Statistical Analyses

The results obtained from the analyses were evaluated using the GraphPad Prism 9.0 statistical software. The Shapiro-Wilk test was performed to assess the normality of data distribution. For comparisons involving multiple groups, one-way analysis of variance (ANOVA) and the Kruskal-Wallis test were used. Post hoc analyses were conducted using the Bonferroni test following ANOVA and the Dunn test following the Kruskal-Wallis test, both of which identified significant differences between variables. A p-value of less than 0.05 was considered statistically significant for all analyses.

Results

Quantification and Characterization of Isolated Exosomes

Nanoparticle tracking analysis (NTA) revealed that the isolated secretomes had an average particle diameter of 81.6 ± 4.2 nm, consistent with the expected size range of exosomes. A representative NTA size distribution image is shown in Figure 1. These findings confirmed the successful isolation of exosome-sized vesicles from the secretomes.

Exosome quantification was performed based on a standard curve generated using exosome solutions with known concentrations. The absorbance of the samples was measured at 405 nm using the ExoCet Exosome Quantitation Kit, and the obtained value was approximately 0.1136 OD. This value was analyzed using the linear regression equation provided by the kit ($y = 0.0012x + 0.0176$; $R^2 = 0.9976$). According to this equation, the exosome concentration in the sample was calculated to be approximately 8×10^7 particles/100 µl.

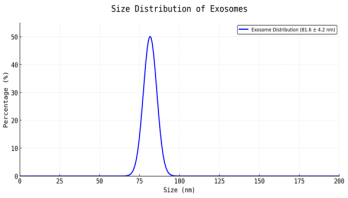

Measurement	Mean Size ± SD (nm)
1st Measurement	79.4 ± 3.9
2nd Measurement	84.1 ± 4.8
3rd Measurement	81.3 ± 3.9
Average	**81.6 ± 4.2**

Figure 1.
Size distribution of isolated exosomes measured by nanoparticle tracking analysis (NTA). Representative histogram showing the size distribution of exosomes (mean ± SD,). The majority of particles were within the 50–150 nm range, consistent with the expected size of exosomes.

Histological Results

Examination of kidney tissues from the control group rats revealed that the glomeruli, cortical, and medullary tubules maintained normal histological structures. Similarly, the Exo-only group exhibited nearly normal histological architecture, with no significant pathological findings except for mild tubular dilation (1.0 [0.0–2.0]) in some specimens. The Cis group, which received cisplatin to induce nephrotoxicity, showed severe pathological changes. These included prominent tubular degeneration (4.0[3.0–4.0]), tubular necrosis (4.0[3.0–4.0]) and tubular dilation (4.0[3.0–4.0]), along with extensive vascular hyperemia (3.0[2.0–4.0]) and collagen/ glycogen accumulation (3.0[2.0–4.0]). These changes indicate widespread structural damage in both parenchymal and stromal regions.

In the group treated with Exo following Cis administration (Cis+Exo group), a substantial reduction in tissue damage was observed compared the Cis group, with notable restoration in stromal and parenchymal areas and only a few degenerated and necrotic cells remaining. Tubular degeneration (1.0[0.0–2.0]), necrosis (0.0[0.0–1.0]), and dilation (1.0[0.0–2.0]) were substantially reduced. Vascular hyperemia (1.0[1.0–2.0]) and collagen/glycogen accumulation (1.0[0.0–2.0]) were also milder. (Figure 2, Table I).

In the PAS-stained sections, the Cis group showed a marked thickening of the glomerular and tubular basement membranes, as well as an increase in glycogen accumulation, indicated by prominent staining in the tubular epithelium. In contrast, the Cis+Exo group exhibited basement membrane thickness and glycogen content comparable to the control groups (Figure 2)

Statistical analysis confirmed that these differences were significant ($p<0.001$ for all parameters). Post-hoc comparisons (b-values) indicated particularly strong significance for tubular degeneration (b = 0.022) and dilation (b = 0.03), while vascular hyperemia (b = 0.352) and collagen/glycogen accumulation (b = 0.054) showed trends toward significance (Table I).

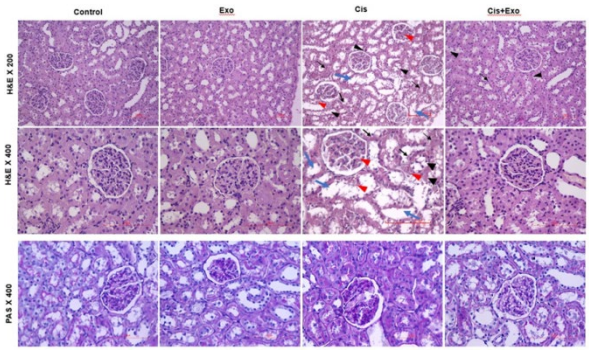

Figure 2.
Representative hematoxylin and eosin (H&E)-stained sections demonstrating the effects of exosome administration on renal tubules and glomeruli (Nikon Eclipse Si, Tokyo, Japan; scale bar: 100 µm). Black arrows indicate necrotic tubular epithelial cells, while arrowheads highlight hydropic degeneration. Blue arrows denote tubular dilatation, and red arrowheads indicate hyperemia observed in both glomerular and intertubular regions. In the lower panel, a representative periodic acid–Schiff (PAS)-stained section (scale bar: 100 µm) is shown.

Table I. Histopathological scoring of kidney tissue.

Group (n=8)	Tubular Degeneration (H&E)	Tubular Necrosis (H&E)	Tubular Dilatation (H&E)	Vascular Hyperemia (H&E)	Collagen/ Glycogen Increase (PAS)
Control	0.0 [0.0–0.0]	0.0 [0.0–1.0]	0.0 [0.0–0.0]	0.0 [0.0–1.0]	0.0 [0.0–1.0]
Exo	0.0 [0.0–1.0]	0.0 [0.0–1.0]	1.0 [0.0–2.0]	0.0 [0.0–1.0]	0.0 [0.0–1.0]
Cis	4.0 [3.0–4.0]	4.0 [3.0–4.0]	4.0 [3.0–4.0]	3.0 [2.0–4.0]	3.0 [2.0–4.0]
Cis+Exo	1.0 [0.0–2.0]	0.0 [0.0–1.0]	1.0 [0.0–2.0]	1.0 [1.0–2.0]	1.0 [0.0–2.0]
p-value	<0.001	<0.001 (b=0.022)	<0.001 (b=0.03)	<0.001 (b=0.352)	<0.001 (b=0.054)

Cis: Cisplatin group; **Exo:** Exosome grup. **b:** Comparison between Cis and Cis+Exo group.

Statistical test: Kruskal–Wallis with Dunn's post hoc test.

Immunohistochemical Results

The aim was to determine the positivity of TGF-β1, α-SMA, and TLR-4, which serve as key markers of fibrosis, in kidney tissues from all experimental groups. Accordingly, areas stained with primary antibodies were photographed. Upon evaluation of the obtained data, the Cis group showed an increased expression of fibrosis markers compared to all other groups. TGF-β1 was strongly expressed in the glomeruli, tubulointerstitial areas, and around blood vessels. α-SMA expression was predominantly observed in the tubulointerstitial regions and around

the glomeruli. TLR-4 expression was mainly detected in the proximal tubules, tubulointerstitial areas, and podocytes of the glomeruli. In the Cis+Exo group, the staining intensity of TGF-β1, α-SMA, and TLR-4 was significantly reduced, indicating decreased expression levels (Figure 3).

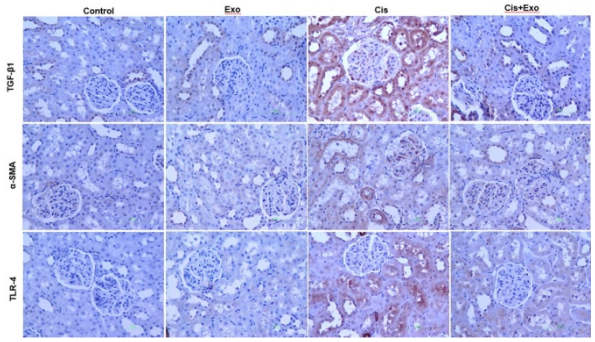

Figure 3.
Immunohistochemical analysis of kidney sections (Nikon Eclipse Si, Tokyo, Japan; X40, scale bar: 100 µm). *Expression patterns of fibrosis-related markers in the kidneys of control and treatment groups. Exosome treatment reduced the expression levels of TGF-β1, α-SMA, and TLR-4 in the kidneys of cisplatin-induced rats. Immunolabeling was performed using the avidin-biotin peroxidase method. TGF-β1: Transforming growth factor beta 1; α-SMA: Alpha-smooth muscle actin; TLR-4: Toll-like receptor 4.*

TGF-β immunoreactivity, showed a significant increase in the Cis group compared to both the Control and Exo groups ($p<0.001$). In the Cis+Exo group, which received Exo treatment after Cis administration, a significant reduction in TGF-β immunoreactivity was observed compared to the Cis group ($p<0.001$). TGF-β promotes the differentiation of fibroblasts into myofibroblasts by increasing α-SMA expression. The expression of α-SMA, was significantly higher in the Cis group compared to the Control and Exo groups ($p<0.001$). Although a significant decrease in α-SMA expression was observed in the Cis+Exo group compared to the Cis group ($p<0.05$), the comparison with the Control group still showed a significant difference ($p<0.001$), indicating that the reduction was not sufficient to reach baseline levels. The TLR-4 marker, also showed a significant increase in the Cis group compared to the Control group ($p<0.001$). A significant decrease in TLR-4 expression was detected in the Cis+Exo group compared to the Cis group (**$p<0.01$). (Figure 4)

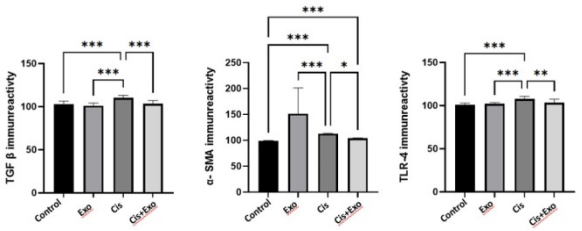

Figure 4.
Immunoreactivity intensity of fibrosis-related proteins. *Effect of Exo on TGF-β, α-SMA, and TLR-4 expression in renal tissue of cisplatin-treated rats. *$p<0.05$, **$p<0.01$, ***$p<0.001$.*

Discussion and Conclusion

Although Cis exhibits strong antitumoral activity and is widely used in the treatment of various types of cancer, it also causes nephrotoxicity[27,28]. Nephrotoxicity is the most significant side effect of cisplatin, observed in 30–40% of treated patients[29]. The histopathological and immunohistochemical findings of this study clearly demonstrated the harmful effects of Cis on kidney tissue through the mechanism of fibrosis. These findings are consistent with previous studies reporting that cisplatin activates apoptosis, autophagy, and inflammatory pathways, leading to irreversible damage in renal cells[27–32]. Commonly reported histological indicators of cisplatin-induced nephrotoxicity include tubular dilatation, cellular necrosis, intraluminal cellular debris, interstitial inflammatory infiltration, and fibrosis.

Numerous studies have demonstrated that bone marrow-derived MSC Exo possesses therapeutic potential for tissue damage and degenerative diseases[33,34]. Depending on their source, Exo vary in content and act as extracellular organelles playing paracrine/endocrine roles by transferring proteins, microRNAs, and enzymes to target cells, thus mediating cell-to-cell communication. MSC-derived Exo have been characterized in many studies for their anti-apoptotic, anti-inflammatory, and regenerative properties[33,35–37].

The chemotherapeutic agent Cis disrupted the kidney histoarchitecture and induced fibrosis. Nephrotoxicity observed in the Cis group was characterized by degenerative changes in the tubular epithelium, necrotic cells, hydropic degeneration, tubular dilatation, and vasculer hyperemia in both glomerular and intertubular regions. Similar histopathological alterations have been reported in other studies investigating nephrotoxicity[27,38,39]. Following a single dose of Exo treatment, a distinct regenerative effect was observed, significantly alleviating nephrotoxicity. Cisplatin-induced fibrosis was associated with the activation of genes promoting fibrosis, leading to an

increase in fibrosis-related proteins. Exosome administration modulated these fibrotic pathways at the genetic level, resulting in a significant reduction in fibrosis protein expression. Furthermore, the findings reported in histopathological scoring, including histopathological improvements in tubular structure, reduction in necrosis and decrease in collagen/glycogen accumulation, support the antifibrotic and protective effects of Exo treatment.

Exo are highly effective paracrine components with significant potential for repairing damaged tissues, playing a critical role in cell-to-cell communication[2-5,24,26]. Exo facilitate intercellular communication by transferring their contents proteins, microRNAs, and enzymes to target cells. Thus, as extracellular organelles, Exo perform paracrine and endocrine functions[40]. Exosomal proteins and microRNAs are functionally complex and are involved in various biochemical and cellular processes, including communication, structural and mechanical functions, inflammation, exosome biogenesis, tissue repair and regeneration, and metabolism[41]. In the present study, Exo treatment substantially reduced tissue damage associated with Cis-induced nephrotoxicity. Since exosome uptake is dependent on intracellular and microenvironmental acidity and since tissue injury is often associated with tissue acidosis Exo are preferentially endocytosed by cells within injured tissues. This suggests that damaged tissues may selectively host Exo[37]. Moreover, the capacity of Exo to trigger appropriate cellular responses during tissue injury is likely influenced by the biochemical potential of their protein and RNA cargo and the maintenance of tissue microenvironment homeostasis[38]. Exo that reach the site of injury have been shown to reduce oxidative stress through their anti-apoptotic, anti-cancer, and antioxidant properties[41,42].

Oxidative stress and tissue acidosis induced by Cis in the kidney tissue activated apoptotic mechanisms. During apoptosis, as cell death occurs, signals released from fragmented cells activate immune cells and fibroblasts, initiating the tissue repair process. However, if cell death becomes chronic or if the inflammatory response is excessive, fibroblasts may overproduce collagen, leading to the replacement of normal tissue with rigid and dysfunctional fibrotic tissue[43]. Previous studies have shown that antitumor agents, including cisplatin, can induce apoptosis and subsequently initiate fibrotic responses through persistent inflammation and tissue remodeling processes[44,45]. In this study, cisplatin-induced fibrosis in the kidney was identified by the increased expression of fibrosis-related proteins such as TGF-β, α-SMA, and TLR-4. A single dose of Exo treatment significantly contributed to tissue repair by modulating the fibrosis induced by Cis. This suggests that Exo can modulate profibrotic pathways, possibly by interrupting TGF-β–mediated signaling cascades, which not only drive myofibroblast activation and ECM accumulation but are also amplified by inflammatory responses that further enhance TGF-β expression[13]. Interestingly, α-SMA immunoreactivity in the Exo-only group was higher than in both the Cis and Cis+Exo groups, as seen in Figure 4. While unexpected, this elevation may reflect a physiological myofibroblast presence involved in homeostatic repair or cytoskeletal remodeling rather than pathological fibrosis. Previous reports suggest that α-SMA can transiently increase during normal tissue regeneration processes, especially under the influence of extracellular vesicles containing growth factors or RNA species[46]. Therefore, the elevated α-SMA in the Exo group might indicate regenerative activation, distinct from the sustained fibrotic remodeling seen in the Cis group. The elevated expression of TLR-4 in the Cis group supports its established role in mediating inflammation-driven fibrosis. By activating downstream NF-κB and TGF-β signaling pathways, TLR-4 amplifies fibrotic responses in the kidney[47], a process that appears to be significantly modulated by Exo treatment in our study.

These observations are consistent with earlier studies demonstrating that MSC-derived exosomes can reduce oxidative stress, suppress proinflammatory cytokines, and modulate fibrotic mediators in kidney injury models[45,48-50]. However, the current study provides direct molecular and histological evidence for the antifibrotic effects of exosomes in a cisplatin-induced nephrotoxicity model. Taken together, these findings highlight the dual role of Exo in mitigating both oxidative and fibrotic damage. Nevertheless, the complex regulatory behavior of markers like α-SMA warrants further investigation to distinguish between regenerative and pathological myofibroblast activation.

This study provides novel and compelling evidence that cisplatin-induced nephrotoxicity extends beyond acute tubular injury, initiating a cascade of events that culminate in progressive fibrotic remodeling a dimension often overlooked in previous in vivo models. Specifically, Exo treatment significantly suppressed oxidative stress-induced tissue damage and attenuated key fibrotic markers such as TGF-β, α-SMA, and TLR-4, indicating a dual mechanism of protection and fibrosis modulation. These results highlight MSC-Exo not only as cytoprotective agents but also as promising antifibrotic therapeutics with potential applications in chronic kidney injury and fibrotic diseases. However, the study is limited by the use of a single animal model and a one-time Exo administration, which may not fully capture the long-term therapeutic potential or dosing dynamics required for clinical translation. Future research should focus on elucidating the molecular pathways underlying the

antifibrotic effects of Exos, optimizing dosing strategies, and evaluating their efficacy in chronic and diverse models of renal fibrosis to better inform their translational potential.

Researcher Contribution Statement:
Idea and design: A.Y., H.T.Y.; Data collection and processing: Ö.C.M, E.K., N.B., Z.B.G., G.Ö.Ö.; Analysis and interpretation of data: H.T.Y., K.T.K.; Writing of significant parts of the article: H.T.Y.
Support and Acknowledgement Statement:
The studies included in this article were supported by Kırşehir Ahi Evran University Scientific Research Project. Project no: TIP.A2.24.006.
Conflict of Interest Statement:
The authors of the article have no conflict of interest declarations.
Ethics Committee Approval Information:
Approving Committee: Kırşehir Ahi Evran Animal Experiments Local Ethics Committee
Approval Date: 07.02.2024
Decision No: 24/030

References

1. van Niel G, D'Angelo G, Raposo G. Shedding light on the cell biology of extracellular vesicles. Nat Rev Mol Cell Biol. 2018;19:213–28. https://doi.org/10.1038/nrm.2017.125.
2. Liu S, Wu X, Chandra S, et al. Extracellular vesicles: Emerging tools as therapeutic agent carriers. Acta Pharm Sin B. 2022;12(10):3822–42. https://doi.org/10.1016/j.apsb.2022.05.002.
3. Chen YF, Luh F, Ho YS, et al. Exosomes: a review of biologic function, diagnostic and targeted therapy applications, and clinical trials. J Biomed Sci. 2024;31:67. https://doi.org/10.1186/s12929-024-01055-0 .
4. Yu H, Feng H, Zeng H, et al. Exosomes: The emerging mechanisms and potential clinical applications in dermatology. Int J Biol Sci. 2024;20(5):1778–95. https://doi.org/10.7150/ijbs.92897.
5. Dai J, Su Y, Zhong S, et al. Exosomes: key players in cancer and potential therapeutic strategy. Signal Transduct Target Ther. 2020;5(1):145. https://doi.org/10.1038/s41392-020-00261-0 .
6. Hall JE. Guyton & Hall Textbook of Medical Physiology. 14th ed. Philadelphia: Elsevier; 2021.
7. Qi L, Luo Q, Zhang Y, et al. Advances in toxicological research of the anticancer drug cisplatin. Chem Res Toxicol. 2019;32(8):1469–86.
8. Gheorghe-Cetean S, Cainap C, Oprean L, et al. Platinum derivatives: a multidisciplinary approach. J Balkan Union Oncol. 2017;22:568–77.
9. Chabner BA, Ryan DP, Paz-Ares L, et al. Antineoplastic agents. In: Hardman JG, Limbird LE, editors. The Pharmacological Basis of Therapeutics. 10th ed. New York: McGraw-Hill; 2001. p. 1432–4.
10. Crona DJ, Faso A, Nishijima TF, et al. A systematic review of strategies to prevent cisplatin-induced nephrotoxicity. Oncologist. 2017;22(5):609–19.
11. Yao X, Panichpisal K, Kurtzman N, Nugent K. Cisplatin nephrotoxicity: a review. Am J Med Sci. 2007;334(2):115–24.
12. Zhou D, Fu H, Zhang L, et al. Tubule-derived Wnts are required for fibroblast activation and kidney fibrosis. J Am Soc Nephrol. 2017;28:2322–36. https://doi.org/10.1681/ASN.2016080902 .
13. Webster AC, Nagler EV, Morton RL, et al. Chronic kidney disease. Lancet. 2017;389:1238–52. https://doi.org/10.1016/S0140-6736(16)32064-5.
14. Sarıbaş GS, Tozak Yıldız H, Gorgulu O. Ellagic acid inhibits TGFβ1/smad-induced renal fibrosis in diabetic kidney injury. Duzce Med J. 2022;24(3):321–7. https://doi.org/10.18678/dtfd.1198021.
15. Wang Y, Xu R, Yan Y, et al. Exosomes-mediated signaling pathway: a new direction for treatment of organ ischemia-reperfusion injury. Biomedicines. 2024;12(2):353. doi:10.3390/biomedicines12020353.
16. Yoon SY, Yoon JA, Park M, et al. Recovery of ovarian function by human embryonic stem cell derived mesenchymal stem cells in cisplatin-induced premature ovarian failure in mice. Stem Cell Res Ther. 2020;11(1):255.
17. Li P, Ou Q, Shi S, Shao C. Immunomodulatory properties of mesenchymal stem cells/dental stem cells and their therapeutic applications. In: Cellular and Molecular Immunology. Vol. 20. Springer Nature; 2023. p. 558–69.
18. Zhang M, Zang X, Wang M, et al. Exosome-based nanocarriers as bio-inspired and versatile vehicles for drug delivery: recent advances and challenges. J Mater Chem B. 2019;7:2421–33. https://doi.org/10.1039/C9TB00170KZ.
19. Fan Z, Jiang C, Wang Y, et al. Engineering exosomes for targeted drug delivery. Nanoscale Horiz. 2022;7:682–714. https://doi.org/10.1039/D2NH00070A.
20. Helwa I, Cai J, Drewry MD, et al. A comparative study of serum exosome isolation using differential ultracentrifugation and three commercial reagents. PLoS One. 2017;12(1):e0170628.
21. Abdel-Latif R, Fathy M, Anwar HA, et al. Cisplatin-induced reproductive toxicity and oxidative stress: ameliorative effect of kinetin. Antioxidants (Basel). 2022;11(5):863. doi:10.3390/antiox11050863.
22. Sezer G, Yay AH, Sarica ZS, Gonen ZB, Onder GO, Alan A, Yilmaz S, Saraymen B, Bahar D. Bone marrow-derived mesenchymal stem cells alleviate paclitaxel-induced mechanical allodynia in rats. J Biochem Mol Toxicol. 2022 Dec;36(12):e23207. doi: 10.1002/jbt.23207. Epub 2022 Sep 2. PMID: 36052563.
23. Antes T, et al. Methods for microvesicle isolation and selective removal. Patent No.: US 9,005,888 B.
24. Bahar D, Gonen ZB, Gumusderelioglu M, et al. Repair of rat calvarial bone defect by using exosomes of umbilical cord-derived mesenchymal stromal cells embedded in chitosan/hydroxyapatite scaffolds. Int J Oral Maxillofac Implants. 2022;37(5):943–50.
25. Gibson-Corley KN, Olivier AK, Meyerholz DK. Principles for valid histopathologic scoring in research. Vet Pathol. 2013;50(6):1007–15. https://doi.org/10.1177/0300985813485099.
26. Kalkan KT, Tozak Yıldız H, Yalçın B, et al. Therapeutic effects of apilarnil, a bee product, on apoptosis and autophagy in cisplatin-induced rat ovarian toxicity. Food Chem Toxicol. 2025;115594. doi:10.1016/j.fct.2025.115594.
27. McSweeney KR, Gadanec LK, Qaradakhi T, et al. Mechanisms of cisplatin-induced acute kidney injury: pathological mechanisms, pharmacological interventions, and genetic mitigations. Cancers. 2021;13(7):1572. https://doi.org/10.3390/cancers13071572.
28. Sueishi K, Mishima K, Makino K, et al. Protection by a radical scavenger edaravone against cisplatin-induced nephrotoxicity in rats. Eur J Pharmacol. 2002;451(3):203–8. https://doi.org/10.1016/S0014-2999(02)02183-1 .
29. Volarevic V, Djokovic B, Jankovic MG, et al. Molecular mechanisms of cisplatin-induced nephrotoxicity: a balance on the knife edge between renoprotection and tumor toxicity. J Biomed Sci. 2019;26(1):25. doi:10.1186/s12929-019-0518-9.

30. Dasari S, Njiki S, Mbemi A, et al. Pharmacological effects of cisplatin combination with natural products in cancer chemotherapy. Int J Mol Sci. 2022;23(3):1532. https://doi.org/10.3390/ijms23031532.
31. Sallam AO, Rizk HA, Emam MA, et al. The ameliorative effects of L-carnitine against cisplatin-induced gonadal toxicity in rats. Pak Vet J. 2021;41(1):147–51. https://doi.org/10.29261/pakvetj/2020.082.
32. Moradi M, Goodarzi N, Faramarzi A, et al. Melatonin protects rats' testes against bleomycin, etoposide, and cisplatin-induced toxicity via mitigating nitro-oxidative stress and apoptosis. Biomed Pharmacother. 2021;138:111481. https://doi.org/10.1016/j.biopha.2021.111481.
33. Lai RC, Yeo RW, Lim SK. Mesenchymal stem cell exosomes. Semin Cell Dev Biol. 2015;40:82–8. https://doi.org/10.1016/j.semcdb.2015.03.001.
34. Chen B, Li Q, Zhao B, et al. Stem cell-derived extracellular vesicles as a novel potential therapeutic tool for tissue repair. Stem Cells Transl Med. 2017;6(9):1753–8. https://doi.org/10.1002/sctm.17-0094 .
35. Xie Y, Chen Y, Zhang L, et al. The roles of bone-derived exosomes and exosomal microRNAs in regulating bone remodelling. J Cell Mol Med. 2017;21(5):1033–41. https://doi.org/10.1111/jcmm.13037.
36. Lai RC, Tan SS, Teh BJ, et al. Proteolytic potential of the MSC exosome proteome: Implications for an exosome-mediated delivery of therapeutic proteasome. Int J Proteomics. 2012;2012:971907. https://doi.org/10.1155/2012/971907.
37. Parolini I, Federici C, Raggi C, et al. Microenvironmental pH is a key factor for exosome traffic in tumor cells. J Biol Chem. 2009;284(49):34211–22. https://doi.org/10.1074/jbc.M109.041152.
38. Sung CY, Hayase N, Yuen PS, et al. Macrophage depletion protects against cisplatin-induced ototoxicity and nephrotoxicity. Sci Adv. 2024;10(30):eadk9878. https://doi.org/10.1126/sciadv.adk9878.
39. Lee B, Kim YY, Jeong S, et al. Oleanolic acid acetate alleviates cisplatin-induced nephrotoxicity via inhibition of apoptosis and necroptosis in vitro and in vivo. Toxics. 2024;12(4):301. https://doi.org/10.3390/toxics12040301.
40. Xie Y, Chen Y, Zhang L, et al. The roles of bone-derived exosomes and exosomal microRNAs in regulating bone remodelling. J Cell Mol Med. 2017;21(5):1033–41. https://doi.org/10.1111/jcmm.13037.
41. Arslan F, Lai RC, Smeets MB, et al. Mesenchymal stem cell-derived exosomes increase ATP levels, decrease oxidative stress, and activate PI3K/Akt pathway to enhance myocardial viability and prevent adverse remodeling after myocardial ischemia/reperfusion injury. Stem Cell Res. 2013;10(3):301–12. https://doi.org/10.1016/j.scr.2013.01.002.
42. Guo X, Zhai J, Xia H, et al. Protective effect of bone marrow mesenchymal stem cell-derived exosomes against the reproductive toxicity of cyclophosphamide is associated with the p38MAPK/ERK and AKT signaling pathways. Asian J Androl. 2021;23(4):386–91. https://doi.org/10.4103/aja.aja_98_20.
43. Wynn TA, Vannella KM. Macrophages in tissue repair, regeneration, and fibrosis. Immunity. 2016;44(3):450–62. https://doi.org/10.1016/j.immuni.2016.02.015.
44. Ye L, Wang D, Yang M, et al. Chemotherapy effect on myocardial fibrosis markers in patients with gynecologic cancer and low cardiovascular risk. Front Oncol. 2023;13:1173838. https://doi.org/10.3389/fonc.2023.1173838.
45. Zhang S, Liu Q, Chang M, et al. Chemotherapy impairs ovarian function through excessive ROS-induced ferroptosis. Cell Death Dis. 2023;14(5):340. https://doi.org/10.1038/s41419-023-05859-0.
46. Brennan MÁ, Layrolle P, Mooney DJ. Biomaterials functionalized with MSC secreted extracellular vesicles and soluble factors for tissue regeneration. Adv Funct Mater. 2020;30(37):1909125. doi:10.1002/adfm.201909125.
47. Vijayakumar G, Latha A, Anil AP, et al. Cell autonomous TLR4 signaling modulates TGF-β induced activation of human cardiac fibroblasts. Heliyon. 2025;11(4): e42452.
48. Yang X, Liu J, Yin Y, et al. MSC-EXs inhibits uranium nephrotoxicity by competitively binding key proteins and inhibiting ROS production. Ecotoxicol Environ Saf. 2025;289:117654. https://doi.org/10.1016/j.ecoenv.2024.117654.
49. Oz Oyar E, Aciksari A, Azak Pazarlar B, et al. The therapeutical effects of damage-specific stress induced exosomes on the cisplatin nephrotoxicity in vivo. Mol Cell Probes. 2022;66:101861. https://doi.org/10.1016/j.mcp.2022.101861.
50. Kang X, Chen Y, Xin X, et al. Human amniotic epithelial cells and their derived exosomes protect against cisplatin-induced acute kidney injury without compromising its antitumor activity in mice. Front Cell Dev Biol. 2022;9:752053. https://doi.org/10.3389/fcell.2021.752053.